ELSEVIER

Chemical Physics 246 (1999) 363–372

Chemical Physics

www.elsevier.nl/locate/chemphys

Photoinduced intramolecular electron transfer in covalently linked porphyrin–triptycene–(bis)quinone diads and triads

Olaf Korth [a], Arno Wiehe [b], Harry Kurreck [b], Beate Röder [a,*]

[a] *AG Photobiophysik, Institut für Physik, Humboldt-Universität zu Berlin, Invalidenstraße 110, D-10115 Berlin, Germany*
[b] *Institut für Organische Chemie, Freie Universität Berlin, Takustraße 3, D-14165 Berlin, Germany*

Received 21 September 1998

Abstract

Intramolecular photoinduced electron transfer (ET) in porphyrin–quinone diads and porphyrin–quinone(Q_A)–quinone(Q_B) triads was investigated in different solvents by means of picosecond fluorescence and transient absorption spectroscopy. Charge separation rates (5×10^9 s^{-1} to $> 1 \times 10^{11}$ s^{-1}) and charge recombination rates are presented and discussed in terms of the Marcus theory. The free enthalpy of the ET compounds varies from 0.52 to 1.2 eV, which led to ET in the normal and inverted region. It is shown that porphyrin–triptycene–*bis*-quinones have to be considered as an acceptor unit, rather than two separated quinone acceptors, due to their electronic coupling. The data show that in the triads, intramolecular photoinduced ET to either the first or the second quinone occurs depending on the energetics of the compounds, which are influenced by the different bridges between donor and acceptor. There is therefore no indication of sequential ET from the porphyrin to one quinone and subsequently to the other. The results are discussed in comparison with previously described investigations of related porphyrin–acceptor–acceptor compounds in the literature. © 1999 Elsevier Science B.V. All rights reserved.

1. Introduction

In recent years, a broad variety of biomimetic model compounds has been synthesised and investigated by different optical methods in order to understand the dependence of ET reactions on the structural properties of the compounds. Moreover, these studies are thought to contribute to a better insight into the ET processes occurring in the primary events in native photosynthesis. In this context, these efforts have been extended to ET reactions including more than one step to reach the final charge-separated state. Attention has been paid in particular to conformational factors which might influence a multistep ET reaction [1–3].

As has been shown by different groups, a broad range of effects connected to the chemical structure of the model system is observed. The aim of this paper is the presentation of results from time-resolved optical spectroscopy of porphyrin–triptycene–quinone diads and porphyrin–triptycene–*bis*-quinone triads. The novel data will be compared with results obtained in investigations of related triads. Conclusions for the realisation of a sequential ET in these kinds of photosynthetic model compounds are drawn.

* Corresponding author. Tel.: +49-30-2093-7625; fax: +49-30-2093-7666; e-mail: roeder@physik.hu-berlin.de

0301-0104/99/$ - see front matter © 1999 Elsevier Science B.V. All rights reserved.
PII: S0301-0104(99)00111-1

2. Materials and methods

2.1. Compounds

The synthesis of the investigated series of compounds has been published [4]. According to the general structural scheme donor–bridge-acceptor, different combinations of these constituents have been synthesised, resulting in 12 different compounds (Fig. 1).

Free base and zinc–tritolylporphyrins have been used as donors. Three different bridge units have been applied to link donors and acceptors. In order to study the difference between structurally similar diads (porphyrin–triptycene–quinones) and triads (porphyrin–triptycene–*bis*-quinones), acceptor units with two quinones or one quinone, the other one being protected, were investigated.

2.2. Experimental

The laser system of the experimental setup for femtosecond transient absorption spectroscopy included a Ti:Sa seed laser (MIRA 900B, Coherent) pumped with an Ar^{+}-ion laser (Innova 306, Coherent) and a regenerative amplifier (Spitfire, Positive Light) pumped with a frequency-doubled Nd:YLF laser (Merlin, Positive Light, 527 nm). The seed pulses ($\tau_{FWHM} = 130$ fs, $E_{pulse} = 7$ nJ, $\lambda = 790$–800 nm, 76 MHz repetition rate) were amplified in the

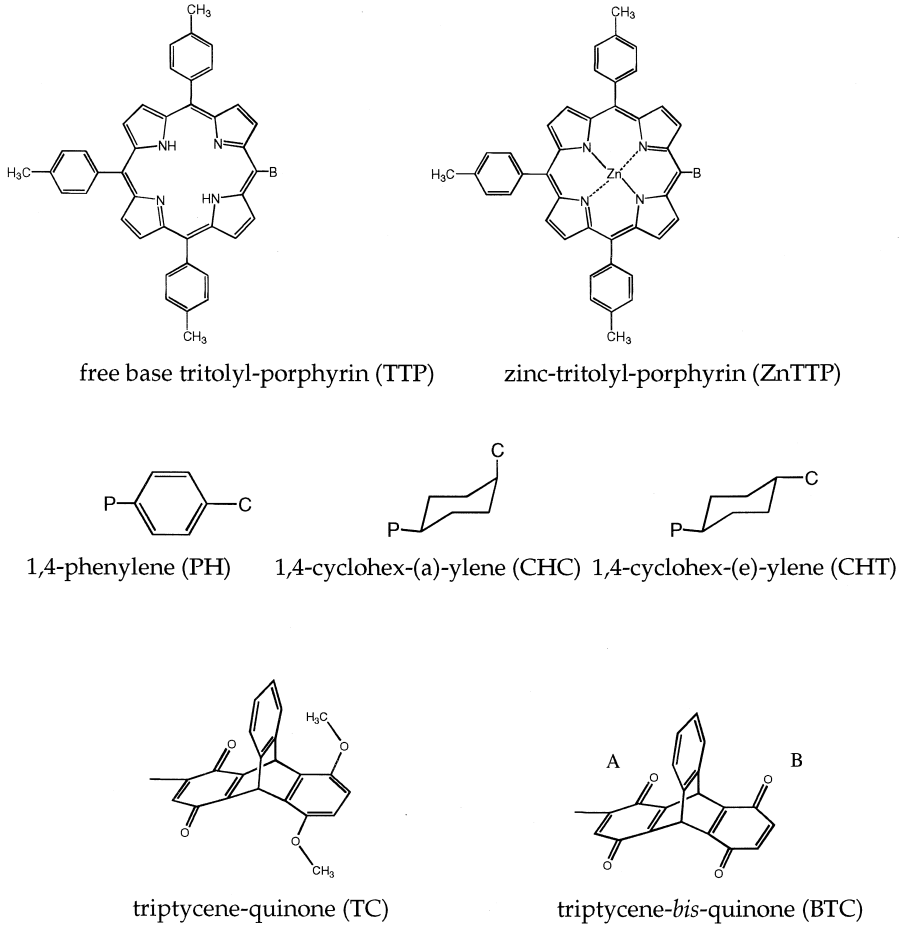

Fig. 1. Donor, bridge and acceptor structures which have been combined in all possible ways given by the donator–bridge-acceptor scheme. This results in the number of twelve ET compounds.

regenerative amplifier up to an energy of about 1 mJ per pulse ($\tau_{FWHM} = 130$ fs, 1 kHz repetition rate). The output of the amplifier was coupled into a second and third harmonic generation (SuperTripler, CSK) or in an optical parametric amplifier (OPA 800, Spectra Physics) to provide excitation light of an appropriate wavelength. A beam splitter was used to split the beam into pump and probe pulses. In the case of second harmonic generation, 70% of the amplifier output was used to generate light of 395–400 nm and 30% white light generation in an ethylene glycol flow-through cell (1 cm). Before generating the white light, the fundamental of the amplifier output passed through a delay line (Newport) which was used to provide a time delay of 7 fs to 1.6 ns between pump and probe pulses. The energy of the probing pulses was $< 5\ \mu J/cm^2$ at the sample. The pump beam had an energy of about 50 μJ per pulse and a spot size of about 2 mm in diameter at the sample. The angle between pump and probe beam was 5–7°. The sample flow-through cell has a path length of 1 mm and was connected to a flow system with a solution reservoir. The white light beam was split into two 50% beams to get test and reference beams. Both beams were coupled into fibre optics after passing the sample cell. The test and reference signals were analysed either with a double CCD-spectrograph (Ocean Optics, SD2000) to get spectral information (420–750 nm) or they were passed through a monochromator ($\Delta\lambda_{FWHM} \approx 5$ nm) and detected with two photomultiplier tubes (H120, Hamamatsu). Shutters were used to block the pump beam for balance measurements and to minimise the irradiation time. The CCD-spectrograph, the delay line and the shutters were driven by a personal computer and appropriate electronics. The home-made LabVIEW© (National Instruments) software allowed the automatic running of a time-series of measurements. Kinetics were extracted from the spectral information at appropriate wavelengths. The rise time of the signal at a single wavelength was about 400 fs.

The time correlated single photon counting (TCSPC) approach was applied for fluorescence lifetime measurements. The apparatus was based on an Ar^+-ion laser pumped, mode-locked titanium:sapphire laser (MIRA 900, Coherent) with a pulse width of 200 fs in the wavelength range of 700–1000 nm. Fluorescence was detected with a microchannel plate photomultiplier (S 3809, Hamamatsu) and integrated electronics (SPC 300, Becker and Hickl). Second harmonic generation was achieved using a BBO crystal. The average power at the sample was 0.5 mW and the illuminated sample area was about 2×2 mm^2. The optical paths for excitation and emission were arranged in a 90° configuration. A monochromator with a spectral width of about 8 nm was used to select the required emission wavelength band. Additional coloured glass filters were used to cut off scattered excitation light. The apparatus response function had a full width of half maximum (FWHM) of 50 ps. Deconvolution of the kinetics was performed with home-made deconvolution software.

3. Results and discussion

3.1. Steady-state optical measurements

The wavelengths and extinction coefficients of the B- and Q-band maxima of covalently linked porphyrin–quinones are given in Table 1.

Neither the wavelengths nor the extinction coefficients of the free base or zinc–porphyrin–quinones vary significantly compared to a free base or zinc–tetratolylporphyrin. The absorption spectra of the porphyrin–quinone compounds are a superposition of the porphyrin and quinone spectra. The quinones have no significant contribution to the absorption spectra and a transient absorption in the spectral range between 400 nm and 750 nm. The observed absorption in this spectral range is attributed to the porphyrin part of the model compounds only.

As shown in Fig. 2, the usual steady-state fluorescence spectra (fluorescence from the S_1 state) of the zinc and free base–ET complexes exhibits no significant difference in the spectral shape and the position of the fluorescence maxima compared to the corresponding tetratolylporphyrins. The maxima of the free base porphyrin fluorescence bands occur in the ranges of 650–657 nm and 720–725 nm. S_1 fluorescence maxima are at about 595–600 nm and 647–655 nm in case of the zinc–porphyrin compounds (in dichloromethane).

Table 1
Wavelength and logarithmic extinction coefficients of the porphyrin–triptycene–(bis)quinone absorption band maxima in dichloromethane ($T = 295$ K)

Compound	B-band λ (nm) (lg ϵ)	Q-bands λ (nm) (lg ϵ)	λ (nm) (lg ϵ)	λ (nm) (lg ϵ)	λ (nm) (lg ϵ)
TTP–PH–TC	418(5.65)	515(4.27)	552(4.03)	591(3.86)	648(3.83)
TTP–PH–BTC	418(5.63)	515(4.25)	552(4.00)	591(3.86)	648(3.79)
TTP–CHC–TC	419(5.61)	517(4.21)	552(3.94)	593(3.68)	649(3.71)
TTP–CHC–BTC	418(5.60)	517(4.20)	552(3.95)	593(3.72)	649(3.72)
TTP–CHT–TC	418(5.63)	517(4.24)	552(3.98)	593(3.70)	649(3.74)
TTP–CHT–BTC	418(5.65)	517(4.24)	552(3.97)	593(3.69)	648(3.71)
ZnTTP–PH–TC	419(5.73)	–	548(4.36)	588(3.93)	–
ZnTTP–PH–BTC	420(5.73)	–	548(4.33)	589(3.79)	
ZnTTP–CHC–TC	420(5.76)	–	550(4.33)	588(3.71)	
ZnTTP–CHC–BTC	420(5.73)	–	550(4.31)	588(3.71)	
ZnTTP–CHT–TC	420(5.73)	–	550(4.31)	588(3.69)	
ZnTTP–CHT–BTC	420(5.71)	–	550(4.34)	587(3.91)	

Interestingly, for some of the zinc–porphyrin derivatives, a fluorescence from the S_2 state was observed by other groups [5–7], as well as for the zinc–porphyrin derivatives described in this paper. The lifetime of the S_2 state was found to be in the order of 1 ps [8]. Kurabayashi et al. [7] obtained a ratio of fluorescence yields for S_1- and S_2-fluorescence of $\phi_F^{S1}/\phi_F^{S2} = 89$ ($\phi_F^{S1} = 3.3 \times 10^{-2}$, $\phi_F^{S2} = 3.7 \times 10^{-4}$) in acetonitrile.

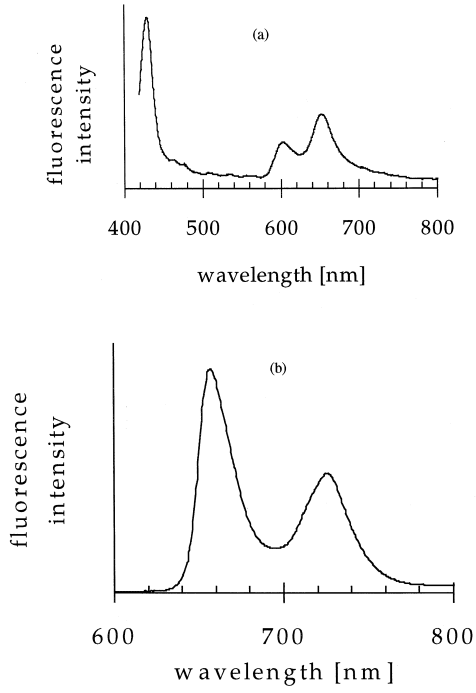

Fig. 2. Fluorescence spectra of: (a) ZnTPP–CHT–BTC; and (b) TPP–CHT–BCT ($c = 2 \times 10^{-6}$ M, $\lambda_{exc} = 405$ nm, $I_{exc} = 1$ mW, in dichloromethane).

However, it is remarkable that in a number of cases of covalently linked zinc–porphyrins, the S_1 fluorescence intensity was even lower than that of the S_2 fluorescence, as shown in Fig. 2(a) for ZnTPP–CHT–BTC. The maximum of the S_2 fluorescence band was observed at 425 nm. These observations led to the following argument.

Owing to the ET, only the fluorescence of the first excited singlet state was strongly quenched. The ET did not affect the S_2 state because of the short S_2 lifetime and the fact that an ET involving the S_2 state of the porphyrin would have a free enthalpy of about 0.85 eV larger than the ET from S_1. This would shift the process far in the inverted region of the Marcus-Theory and reduce the rate dramatically. Consequently, the ratio between the yields of S_1- and S_2-fluorescence became smaller due to the ET.

3.2. ET parameters

The redox potentials were determined from electrochemical measurements (CV). The center-to-center distances of the ET compounds were determined from X-ray structures and Quanta–Charm calculations.

From the listed electrochemical data in Table 2 it can be seen that the free enthalpy of the ET reactions

Table 2
Oxidation (E_{ox}) and reduction ($-E_{red}$) potentials, free enthalpy of the ET reactions ($-\Delta G_{et}$) and donor–acceptor center-to-center distances (R_{da}) of the compounds

Compound	E_{ox} (eV)	$-E_{red}^{(a)}$ (eV)	$-E_{red}^{(b)}$ (eV)	$R_{da}(Q_A)$ (Å)	$R_{da}(Q_B)$ (Å)	$-\Delta G_{et}(Q_A)$ (eV)	$-\Delta G_{et}(Q_B)$ (eV)
TTP–PH–TC	0.97	0.46	–	10.7	–	0.64	–
TTP–PH–BTC	0.99	0.32	0.45	10.7	13.5	0.76	0.60
TTP–CHC–TC	0.93	0.56	–	9.0 (8.3)	–	0.60	–
TTP–CHC–BTC	0.92	0.62	0.38	9.0 (8.3)	13.4 (9.7)	0.55	0.73
TTP–CHT–TC	0.93	0.55	–	10.6	–	0.58	–
TTP–CHT–BTC	0.92	0.62	0.38	10.6	13.4	0.52	0.73
ZnTTP–PH–TC	0.76	0.42	–	10.7	–	1.08	–
ZnTTP–PH–BTC	0.76	0.30	0.53	10.7	13.5	1.20	0.94
ZnTTP–CHC–TC	0.71	0.56	–	9.0 (8.3)	–	1.02	–
ZnTTP–CHC–BTC	0.71	0.64	0.37	9.0 (8.3)	13.4 (9.7)	0.94	1.15
ZnTTP–CHT–TC	0.71	0.57	–	10.6	–	0.98	–
ZnTTP–CHT–BTC	0.70	0.61	0.38	10.6	13.4	0.95	1.15

in the 12 compounds varied from 0.52 to 1.2 eV. It is also shown that the center-to-center distance of different donors and acceptors ranged from about 9 to 13.5 Å.

Owing to the electronic interaction of the different bridges and acceptors, it is important to realise that, assuming a possible sequential ET in the triads from the donor to the nearby quinone, the ET in the 1,4-phenylene-linked compounds would include a down-hill and a following up-hill step. However, in the 1,4-cyclohexylene-linked compounds two down-hill steps would occur. This different behaviour of the two types of porphyrin–quinones can easily be understood, taking into account the different energies of the electronic states. The following results of the electrochemical measurements can be listed as presumptions for the discussion of ET reactions in the porphyrin–triptycene–quinones:

- The energies of the charge-separated states of the triads are different from those of the corresponding diads.
- The energies of the charge-separated states of the triads are affected by the nature of the bridge between porphyrin and quinone, due to the different electronic properties of the bridges.
- The free enthalpy of the ET reactions varies from 0.52 to 1.20 eV.
- Zinc–porphyrin complexes generally exhibit larger free enthalpies of the ET reaction compared to free base porphyrins.
- The free enthalpy of the ET to Q_A is smaller in the 1,4-cyclohexylene-linked triads than that in the diads.
- In the 1,4-phenylene-linked compounds, the free enthalpy of the ET to Q_A is larger in the triads than in the diads.

3.3. Time resolved fluorescence spectroscopy

In Table 3, the results of time-resolved fluorescence measurements are listed. The obtained fluorescence decays were fitted using biexponential functions for the decay of the diads and a sum of three exponential functions for the triads. The three exponential model was used since biexponential fits did not describe the data sufficiently well. This was deduced from the chi square parameter (χ^2) of the fits. Comparison of the obtained decay times of the multi-exponential fits with the decay times of the free base- and zinc–tetratolylporphyrins reveals that the fluorescence decay component of ca. 7.6 ns is caused by porphyrins with 'inactive' quinones (e.g. hydroquinones). Careful optimisation of the experimental conditions enables the amount of the decay component of the porphyrin–hydroquinones to be kept to less than 5% during the experiment. The first component of the fluorescence decays of the diads as well as the first and second components of the fluorescence decays of the triads are due to different intramolecular ET reactions in the model compounds. Owing to the limited time resolution (ca. 10

Table 3
Results of the time resolved fluorescence measurements and calculated rate constants[a] of ET reactions ($\lambda_{exc} = 420$ nm, $I_{exc} = 1.5$ mW, $E_{pulse} = 20$ pJ, $t_{pulse} = 200$ fs, $\lambda_{em} = 650$ nm, $c = 1 \times 10^{-6}$ M, $T = 295$ K)

Compound	τ_1 (ps)	τ_2 (ps)	τ_3 (ps)	$k_{et(A)}$ (10^{10} s^{-1})	$k_{et(B)}$ (10^{10} s^{-1})
TTP–PH–TC	$<=11$	–	7.7 ± 0.3	>9.0	–
TTP–PH–BTC	$<=10$	770 ± 100	7.5 ± 0.3	>10.0	0.12
TTP–CHC–TC	60 ± 10	–	7.5 ± 0.3	1.6	–
TTP–CHC–BTC	21 ± 5	850 ± 150	7.6 ± 0.3	0.10	4.7
TTP–CHT–TC	52 ± 10	–	7.7 ± 0.3	1.9	–
TTP–CHT–BTC	20 ± 5	900 ± 200	7.5 ± 0.3	0.098	5.0
ZnTTP–PH–TC	51 ± 10	–	1.6 ± 0.3	1.9	–
ZnTTP–PH–BTC	59 ± 10	965 ± 100	1.8 ± 0.3	1.6	0.045
ZnTTP–CHC–TC	13 ± 5	–	1.7 ± 0.3	7.6	–
ZnTTP–CHC–BTC	23 ± 5	260 ± 50	1.6 ± 0.3	0.37	4.3
ZnTTP–CHT–TC	12 ± 5	–	1.8 ± 0.3	8.3	–
ZnTTP–CHT–BTC	23 ± 5	270 ± 50	1.8 ± 0.3	0.36	4.3

Because of the difference of the higher free enthalpy of the ET for the reaction involving Q_A in case of the 1,4-phenylene linked compounds and Q_B in case of the 1,4-cyclohexylene linked compounds, the rate $k_{et(A)}$ is higher than $k_{et(B)}$ for the 1,4-phenylene linked compounds and lower than $k_{et(B)}$ for the 1,4-cyclohexylene linked compounds.

ps after deconvolution), in some cases only an upper limit of the decay time can be estimated.

A reasonable interpretation of the experimental results can be given within the framework of the Marcus theory. The data of both, the diads and triads, are well fitted by the semiclassical Marcus equation:

$$k_{et} = \frac{2\pi}{\hbar} H_{RP}^2 (4\pi\lambda_B T)^{-1/2} \exp\left[-\frac{(\lambda + \Delta G^0)^2}{4\lambda k_B T} \right]. \quad (1)$$

Owing to their different energetics, the ET compounds can be separated into two groups. The first group includes all 1,4-phenylene-bridged compounds and the second group includes all 1,4-cyclohexylene-bridged compounds. The fitting parameters are the reorganisation energy λ and the matrix element H_{RP}. All other parameters are taken from the experimental data.

The ET with the larger reaction enthalpy is in either of these two groups assigned to the highest ET rate observed for a triad, regardless of the distance between the involved quinone acceptor and the donor. The free enthalpy dependence of the ET on the quinone that is harder to reduce in the triads has to be fitted separately. Although the number of data points was limited, the available data were again described well by the semiclassical Marcus equation. In the case of free base porphyrin compounds, the rate constant increased with the free enthalpy of the ET reaction. The opposite tendency was observed for the zinc–porphyrin–quinones, namely, a decrease of the rate constant with increasing free enthalpy. This different behaviour can be explained by the fact that in case of the zinc–porphyrin–quinones the ET reaction occurs in the inverted region, whereas the ET in free base porphyrin–quinones can adequately be described by the normal region characteristics (Table 3, Fig. 4).

Since the triads have two quinone acceptors a two-step ET could be expected for these compounds. Assuming sequential ET, the first step of ET to Q_A would be the fluorescence decay determining step and a second decay component should not be observed. However, two short decay components could be detected in time-resolved fluorescence experiments for all triads investigated. On the contrary, only one short decay component was observed for all diads. On the other hand, a sequential two-step ET in 1,4-phenylene-linked triads would require an activation enthalpy of approximately 250 meV for the second step. Thus, even at room temperature the process is very unlikely to occur. For the 1,4-cyclohexylene-linked compounds a sequential two-step ET is favoured, because in this case both steps are exergonic. Fig. 3 illustrates this situation for diads and triads with different bridges.

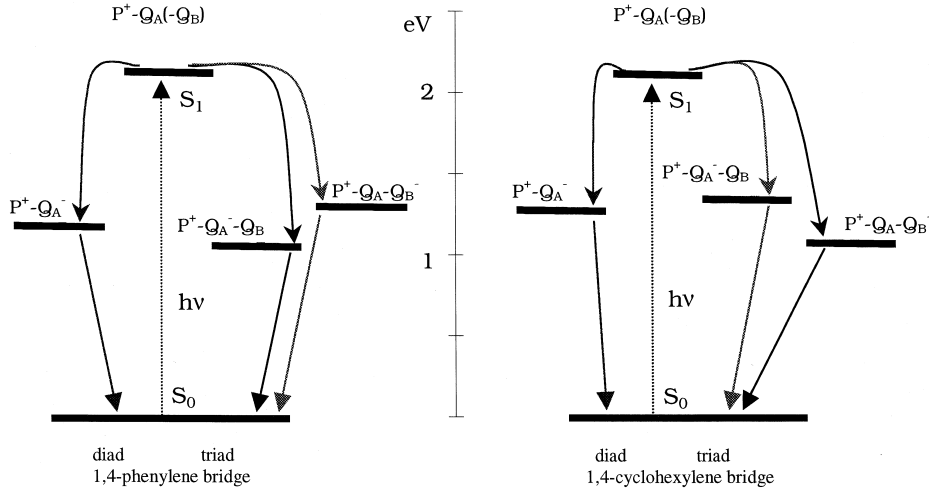

Fig. 3. Energy scheme of the ET reactions in porphyrin–triptycene–(bis)quinone diads (one of the quinones protected) and triads with different bridges between donor and acceptor.

Taking into account the energetics (Fig. 3) and data analysis in the framework of the Marcus-Theory, an unambiguous interpretation requires the consideration of ET reactions either to Q_A or to Q_B directly.

The observed behaviour in Fig. 4 shows that in case of the 1,4-phenylene bridge, the larger ET rate has to be assigned to the transfer to Q_A. Considering Table 3, it becomes obvious that the free base porphyrin compounds with 1,4-phenylene bridges exhibit normal region properties. However, the 1,4-phenylene linked zinc–porphyrin compounds are clearly in the inverted region. This observation does not depend on whether the electron is transferred to Q_A or to Q_B.

In case of a 1,4-cyclohexylene bridge the larger ET rate has to be assigned to an ET from the porphyrin to Q_B. The ET processes to Q_B in ZnTTP–CHT–BTC and ZnTTP–CHC–BTC again show inverted region behaviour. This finding holds regardless of whether the electron is transferred to Q_A or Q_B.

It can also be seen that the ET drops significantly if, in case of the 1,4-phenylene bridge, Q_B or, for the

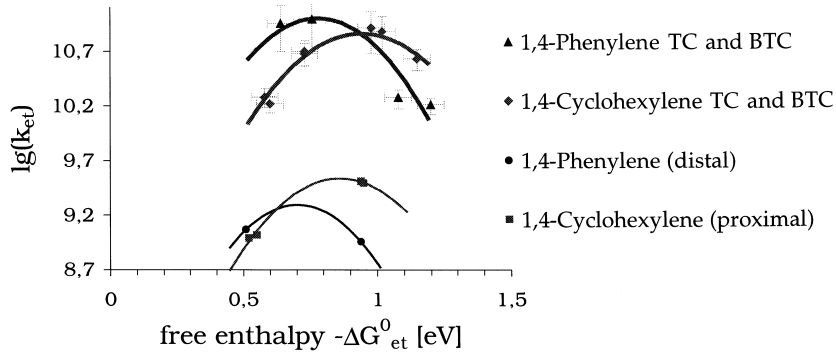

Fig. 4. Free enthalpy dependence of the ET rate. The compounds are assigned to four groups due to their different bridges and the different position of the easier reducible quinone acceptor. The data for the groups are fitted separately with the semiclassical Marcus-equation.

1,4-cyclohexylene bridge, Q_A is involved. This is due to the smaller free enthalpy of these ET pathways. The obtained data indicate that the free enthalpy is the determining factor for the magnitude of the rate constant, rather than the distance between donor and acceptor. In both groups, the 1,4-phenylene- as well as the 1,4-cyclohexylene-bridged compounds, the reorganisation enthalpy for the process involving the weaker acceptor is 80 meV lower than that of the ET to the stronger acceptor (Table 4). The presented numbers in Table 4 were obtained from a data analysis using the semiclassical Marcus equation.

The quantum yield of the ET is mostly $> 90\%$. The reorganisation enthalpy vary from 0.70 to 0.94 eV. These values are very similar to what has been observed for related compounds [9]. The calculated activation enthalpies are in the range of thermal energies at room temperature. The data analysis allows the estimation of the matrix elements of the electronic coupling H_{RP}^2. The calculated values range from 10 to 25 cm^{-1} for the diads and the ET to the stronger acceptor in the triads. For the ET to the weaker acceptor in the triads the values for H_{RP} amount to 2–5 cm^{-1}. Consequently, non-adiabatic ET occurs in all cases. Concerning the effect of the electronic coupling between the two acceptors, the porphyrin–triptycene–*bis*-quinones can be compared to related compounds, thus allowing a qualitative discussion of structural properties on the nature of the ET. Staab and co-workers [1,3,10–13] characterised the ET of porphyrin–cyclophane–quinone–quinone compounds (Fig. 6). They found that the two quinones have to be considered as one acceptor unit rather than two separated acceptors. This is due to the coupling of the electronic systems of the quinones in this conformation. Furthermore, it has been shown that the ET occurs only between the porphyrin donor and the outer quinone, which is the stronger acceptor. Thus a one-step ET occurs in this system.

The opposite situation was observed by Ohkohchi et al. [2]. They investigated porphyrin–pyromellitimide–quinone triads. Using transient absorption spectroscopy, they showed that two sequential ET steps take place, where the electron is located first at the inner acceptor and than at the outer acceptor. The arrangement of the two acceptors disfavours any electronic coupling of the acceptors.

Considering the porphyrin–triptycene–*bis*-quinone triads which were investigated in this paper, obviously the intermediate electronic coupling of the two quinone acceptors leads to a situation somewhat in between the two limits represented by the compounds of Staab and co-workers [1,3,10–13] and Ohkohchi et al. [2]. Instead of a dominant acceptor or a sequential ET, an ET either to Q_A or to the other quinone Q_B takes place. The different rates are mainly determined by the free enthalpy of the reaction. The free enthalpy depends on the position of the quinone (inner or outer part of the acceptor unit, relative to the donor). This is established by electro-

Table 4
Quantum yields (Φ_{et}), reorganization energies (λ) and activation energies (ΔG_{et}^*) of ET reactions of porphyrin–triptycene–(bis)quinones

Compound	$\Phi_{et(A)}$	$\Phi_{et(B)}$	$\lambda_{(A)}$ (eV)	$\lambda_{(B)}$ (eV)	$\Delta G_{et(A)}^*$ (meV)	$X_{et(A)}^*$ (meV)
TTP–PH–TC	0.99	–	0.78	–	6	–
TTP–PH–BTC	≈ 1.0	0.92	0.78	0.70	0	4
TTP–CHC–TC	0.96	–	0.94	–	31	–
TTP–CHC–BTC	0.85	0.99	0.86	0.94	28	12
TTP–CHT–TC	0.99	–	0.94	–	34	–
TTP–CHT–BTC	0.88	≈ 1.0	0.86	0.94	34	12
ZnTTP–PH–TC	0.97	–	0.78	–	**29***	–
ZnTTP–PH–BTC	0.94	0.43	0.78	0.70	**57***	**21***
ZnTTP–CHC–TC	0.99	–	0.94	–	2	–
ZnTTP–CHC–BTC	0.96	0.99	0.94	0.86	**2***	**12***
ZnTTP–CHT–TC	≈ 1.0	–	0.94	–	0	–
ZnTTP–CHT–BTC	0.96	0.99	0.94	0.86	**2***	**12***

Bold printed activation energies (*) are assigned to ET reactions in the inverted region.

Table 5
Fluorescence decay times, ET rates and quantum yields of the ET reactions of free base porphyrin–1,4-cyclohexylene compounds in 1,2-dimethoxyethane ($\lambda_{exc} = 420$ nm, $I_{exc} = 1.5$ mW, $E_{pulse} = 20$ pJ, $t_{pulse} = 200$ fs, $\lambda_{em} = 650$ nm, $c = 1 \times 10^{-6}$ M, $T = 295$ K)

Compound	τ_1 (ps)	τ_2 (ps)	$k_{et(A)}$	$k_{et(B)}$	$\Phi_{et(A)}$	$\Phi_{et(B)}$
TTP–CHC–TC	321 ± 20	–	3.0×10^9	–	0.96	–
TTP–CHC–BTC	132 ± 20	430 ± 50	2.2×10^9	7.5×10^9	0.95	0.99
TTP–CHT–TC	356 ± 20	–	2.7×10^9	–	0.96	–
TTP–CHT–BTC	107 ± 20	480 ± 50	2.0×10^9	9.2×10^9	0.96	0.99

chemical data (Table 2) and explained in terms of the influence of the bridge between donor and acceptor unit, mainly that at the inner acceptor (Fig. 3).

Investigations in different solvents confirm the observed behaviour that was observed in dichloromethane. Time-resolved fluorescence measurements were also carried out in dimethylformamide (DMF), toluene and 1,2-dimethoxyethane. The results for the free base porphyrin–1,4-cyclohexylene compounds in 1,2-dimethoxyethane are shown in Table 5. Again, two ET rates were obtained for triads. The smaller ET rates compared to dichloromethane might be connected to a change in the energetics of the systems due to solvent changes or the intrinsic solvent properties.

3.4. Transient absorption

Further confirmation was given by transient absorption measurements. Because of the instability of the compounds under UV light irradiation in dichloromethane ($\lambda_{exc} = 390$ nm, $\tau_{pulse} = 130$ fs, $E_{pulse} = 50$ μJ), the transient absorption experiments had to be carried out in DMF. Spectra in the range of 420 to 750 nm were recorded in the time range of 0–1.6 ns. A global data analysis in this spectral range was performed. In agreement with the fluorescence measurements of the triads, a reasonable fit of decays at different wavelength in the whole spectral range required a model with two distinguished ET reactions in case of the triads. No absorption of the charge separated state could be observed in these experiments. The fit of the porphyrin-S_1 state decay was performed using a biexponential model function:

$$\Delta OD(\lambda,t) = a_0(\lambda) + a_1(\lambda)\exp\left(-\frac{t}{\tau_1}\right) + a_2(\lambda)\exp\left(-\frac{t}{\tau_2}\right), \quad (2)$$

where λ is the observation wavelength, t is the delay time after excitation, the constant a_0 represents the approximately constant part (in the given time range) of the transient absorption signal resulting from the

Table 6
S_1-decay times and ET rates of four free base porphyrin–triptycene–(bis)quinones in DMF, calculated from time series of ΔOD-Spectra

Compound	τ_1 (ps)	τ_2 (ps)	$k_{et(A)}$ (10^{10} s^{-1})	$k_{et(B)}$ (10^{10} s^{-1})
TTP–PH–TC	10.5 ± 1	–	9.5	–
TTP–PH–BTC	7.8 ± 1	300 ± 100	12.8	0.32
TTP–CHT–TC	60 ± 10	–	1.6	–
TTP–CHT–BTC	35 ± 5	250 ± 50	0.39	3.8

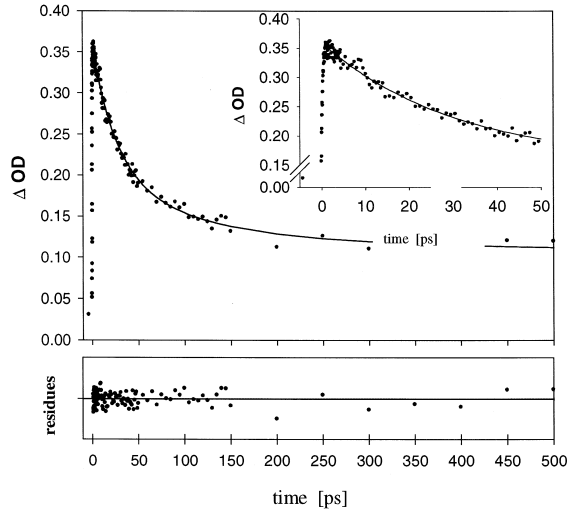

Fig. 5. Transient absorption decay of the S_1 state of TTP–CHT–BTC in DMF at $\lambda_{abs} = 446$ nm, $\tau_1 = 35 \pm 5$ ps (55%), $\tau_2 = 250 \pm 50$ ps (15%), a_0 (30%). ($T = 295$ K, $\lambda_{exc} = 390$ nm, $\tau_{pulse} = 130$ fs (FWHM), $E_{pulse} = 50$ μJ).

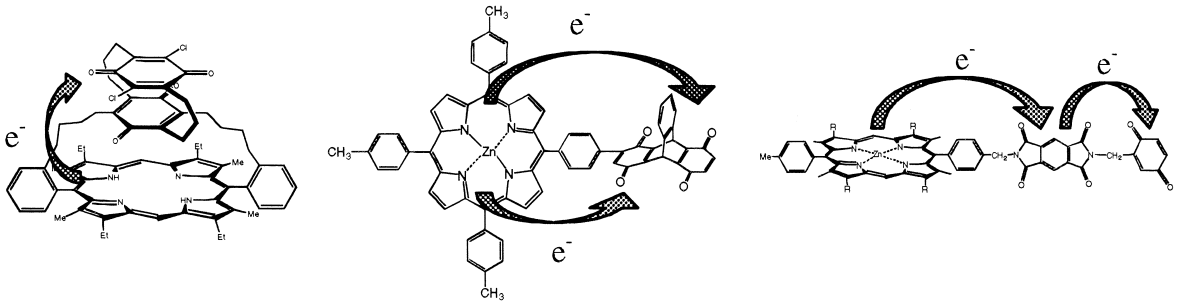

Fig. 6. Structures of: (a) a porphyrin–cyclophane–quinone–quinone triad (after Staab et al. [10]); (b) ZnTTP–PH–BTC (after Wiehe et al. [4]); and (c) a porphyrin–pyromellitimide–quinone triad (after Ohkohchi et al. [2]).

S_1 state and triplet absorption of not oxidised porphyrins (for instant due to hydroquinones) and τ_1 and τ_2 represent the ET times of the transfer to either Q_A or Q_B (Table 6). A reasonable fit (Fig. 5) of the triad S_1 state decay could be attained only if two exponential components were used.

Owing to the change of the solvent, the larger and smaller rate constants changed differently, depending on whether the inner or the outer quinone was involved. The higher ET rates were comparable to the rates which were observed in dichloromethane.

The authors are aware of the differences between these investigations at room temperature (singlet transfer) and low temperature ESR-measurements (triplet transfer) of the same compounds. Nevertheless, it seems to be remarkable that in both cases two different charge separated states ($P^{\cdot+}$–$Q_A^{\cdot-}$–Q_B or $P^{\cdot+}$–Q_A–$Q_B^{\cdot-}$) are observed for the triads [14] (see Fig. 6).

In conclusion, two remarkable factors have to be considered for ET model compounds like porphyrin–triptycene–*(bis)*quinones: (1) the influence of the bridge between donor and acceptor at the free enthalpy of the ET in given molecular system; and (2) the fact that the electronic coupling of the two acceptors, in case of the triads, leads to either an ET to Q_A or Q_B.

Acknowledgements

The authors like to thank Dr. habil. M.O. Senge for the center-to-center distance data from X-ray structures of ZnTTP–PH–TC and Dr. J. Sobek for the cyclovoltammetric measurements. The transient absorption experiments were carried out in Prof. Dr. M.A.J. Rodgers (Bowling Green State University, Ohio) laboratories. O.K. would like to thank Prof. Dr. M.A.J. Rodgers for his support. The work was supported by VW-Stiftung (Gr. Nr. I/72382).

References

[1] H.A. Staab, M. Tercel, R. Fischer, C. Krieger, Angew. Chem. 106 (1994) 1531.
[2] M. Ohkohchi, A. Takahashi, N. Mataga, T. Okada, A. Osuka, H. Yamada, K. Maruyama, J. Am. Chem. Soc. 115 (1993) 12137.
[3] F. Pöllinger, H. Heitele, M.E. Michel-Beyerle, M. Tercel, H.A. Staab, Chem. Phys. Lett. 209 (1993) 251.
[4] A. Wiehe, M.O. Senge, H. Kurreck, Liebigs Ann. Recueil (1997) 1951.
[5] L. Bajema, M. Gouterman, J. Mol. Spectrosc. 39 (1971) 421.
[6] S. Tobita, Y. Kaizu, H. Kobayashi, I. Tanaka, J. Chem. Phys. 81 (1984) 2962.
[7] Y. Kurabayashi, K. Kikuchi, H. Kokubun, Y. Kaiz, H. Kobayashi, J. Phys. Chem. 88 (1984) 1308.
[8] H. Chosrowjan, S. Tanigichi, T. Okada, S. Takagi, T. Arai, K. Tokumaru, Chem. Phys. Lett. 242 (1995) 644.
[9] M.R. Wasielewski, Chem. Rev. 92 (1992) 435.
[10] H.A. Staab, G. Voit, J. Weiser, M. Futscher, Chem. Ber. 125 (1992) 2303.
[11] H.A. Staab, J. Weiser, E. Baumann, Chem. Ber. 125 (1992) 2275.
[12] C. Krieger, M. Dernbach, G. Voit, T. Carell, H.A. Staab, Chem. Ber. 126 (1993) 811.
[13] W. Frey, R. Klann, F. Laermer, T. Elsaesser, E. Baumann, M. Futscher, H.A. Staab, Chem. Phys. Lett. 190 (1992) 567.
[14] G. Elger, H. Kurreck, A. Wiehe, E. Johnen, M. Fuhs, T. Prisner, J. Vrieze, Acta Chem. Scand. 51 (1997) 593.